

# Journal Pre-proof

Nystagmus and optical coherence tomography findings in *CNGB3*-associated achromatopsia

Nashila Hirji, MBBS, FRCOphth, Maria Theodorou, PhD, FRCOphth, James W. Bainbridge, PhD, FRCOphth, Nadia Venturi, Michel Michaelides, MD(Res), FRCOphth

PII: S1091-8531(20)30050-1

DOI: <https://doi.org/10.1016/j.jaapos.2019.11.013>

Reference: YMPA 3154

To appear in: *Journal of AAPOS*

Received Date: 1 August 2019

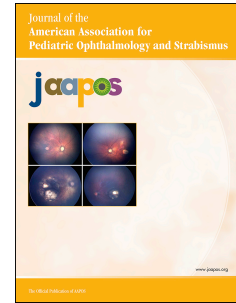
Revised Date: 13 November 2019

Accepted Date: 24 November 2019

Please cite this article as: Hirji N, Theodorou M, Bainbridge JW, Venturi N, Michaelides M, Nystagmus and optical coherence tomography findings in *CNGB3*-associated achromatopsia, *Journal of AAPOS* (2020), doi: <https://doi.org/10.1016/j.jaapos.2019.11.013>.

This is a PDF file of an article that has undergone enhancements after acceptance, such as the addition of a cover page and metadata, and formatting for readability, but it is not yet the definitive version of record. This version will undergo additional copyediting, typesetting and review before it is published in its final form, but we are providing this version to give early visibility of the article. Please note that, during the production process, errors may be discovered which could affect the content, and all legal disclaimers that apply to the journal pertain.

Copyright © 2020, American Association for Pediatric Ophthalmology and Strabismus. Published by Elsevier Inc. All rights reserved.



## **Nystagmus and optical coherence tomography findings in *CNGB3*-associated achromatopsia**

Nashila Hirji, MBBS, FRCOphth,<sup>a,b</sup> Maria Theodorou, PhD, FRCOphth,<sup>a,b</sup> James W. Bainbridge, PhD, FRCOphth,<sup>a,b</sup> Nadia Venturi,<sup>b</sup> and Michel Michaelides, MD(Res), FRCOphth<sup>a,b</sup>

*Author affiliations:* <sup>a</sup>UCL Institute of Ophthalmology, University College London, London, United Kingdom; <sup>b</sup>Moorfields Eye Hospital, London, United Kingdom

*Supported by grants from MeiraGTx, the National Institute for Health Research Biomedical Research Centre at Moorfields Eye Hospital NHS Foundation Trust and UCL Institute of Ophthalmology, Medical Research Council, Fight for Sight (UK), Moorfields Eye Hospital Special Trustees, Moorfields Eye Charity, Retina UK, and the Foundation Fighting Blindness (USA).*

*Disclosures:* Michel Michaelides and James Bainbridge consult for MeiraGTx.

*Submitted August 1, 2019.*

*Revision accepted November 27, 2019.*

*Correspondence:* Maria Theodorou, Paediatric Ophthalmology and Strabismus Service, Moorfields Eye Hospital, 162 City Road, London EC1V 2PD, UK (email: mtheodorou@nhs.net).

**Word count: 3,230**

**Abstract only: 196**

## **Abstract**

### *Purpose*

To describe the nystagmus characteristics of subjects with molecularly confirmed *CNGB3*-associated achromatopsia and report the spectral domain optical coherence tomography (SD-OCT) findings in these individuals.

### *Methods*

Adults and children with *CNGB3*-achromatopsia underwent visual acuity testing, ocular motility assessments, video nystagmography, and SD-OCT imaging. Qualitative assessment of foveal structure was performed by grading SD-OCT images into one of five categories.

### *Results*

A total of 18 subjects (11 adults) were included. The majority demonstrated a phoria, with manifest strabismus present in only 3 subjects. The predominant nystagmus waveform within the cohort was pure pendular. Nine individuals demonstrated a mixture of waveforms. Nystagmus frequencies were 4-8 cycles/second, with no notable differences in eye movements between adults and children. SD-OCT imaging revealed a continuous ellipsoid zone (EZ) at the fovea in 2 subjects (grade 1) and EZ disruption (grade 2) in the remaining 16. Retinal structure characteristics were symmetrical in both eyes in each subject.

### *Conclusions*

In our study cohort, nystagmus in *CNGB3*-associated achromatopsia had distinctive features, and the majority of subjects had retinal abnormalities at the fovea on SD-OCT. Early use of SD-OCT in the clinical work-up may eliminate the need for more invasive investigations, such as neuro-imaging.

Infantile nystagmus syndrome (INS) usually manifests by 3-6 months of age and has a prevalence of approximately 14 per 10,000.<sup>1</sup> It may be idiopathic or associated with ocular or systemic pathology. Ocular causes include congenital cataracts, optic nerve hypoplasia, and retinal diseases, such as achromatopsia and albinism.<sup>2</sup>

Although history and examination may be strongly suggestive of the etiology of nystagmus, magnetic resonance imaging (MRI) is often used in cases where presentation is atypical (eg, with a vertical or torsional element) to exclude a neurological cause.<sup>3</sup> Ocular pathologies (in particular, inherited retinal disorders) are more frequently associated with INS than is neurological disease<sup>4</sup>; thus, detailed assessment of the nystagmus and retina may obviate the need for neuroimaging in infants and young children.

Optical coherence tomography (OCT) has been advocated for first-line imaging investigation in INS, and the development of handheld spectral domain OCT (SD-OCT) has enabled the identification of retinal pathology in infants and young children with INS.<sup>5,6</sup> Thus, SD-OCT may aid in the early assessment and stratification of young patients with retinal disease for potential therapeutic intervention.<sup>7</sup> This is relevant for achromatopsia, for which early intervention may yield better outcomes.<sup>8,9</sup> The current study presents nystagmus characteristics as well as SD-OCT findings in a cohort of adults and children with achromatopsia.

### **Subjects and Methods**

Adults and children with achromatopsia secondary to likely disease-causing variants in the *CNGB3* gene were included. All subjects were participants in an unmasked clinical trial at Moorfields Eye Hospital assessing gene therapy in *CNGB3*-associated achromatopsia and were drawn from a cohort of approximately 80 individuals taking part in an achromatopsia natural history study. Only individuals with evidence of relative preservation of cone photoreceptors on

SD-OCT imaging were included, because it was anticipated that such subjects would be the most likely to benefit from gene supplementation.<sup>8</sup> In addition, subjects <30 years of age were prioritized, because it was felt that younger individuals would receive optimum benefit from treatment. The study adhered to the tenets of the Declaration of Helsinki and was approved by the Moorfields Eye Hospital Ethics Committee. Informed consent was obtained from all adult subjects prior to entering the study; informed consent and assent were obtained from parents and children (<16 years of age).

A full ophthalmic assessment of all participants was conducted at baseline, including slit-lamp examination of the anterior and posterior segments. All subjects had baseline visual acuity testing, ocular motility assessments, nystagmography, and SD-OCT scans between January 2017 and November 2018.

#### *Nystagmography*

Eye movements (monocular and binocular) of all subjects were recorded using an EyeLink 1000 video-based eye tracker (SR Research, Mississauga, ON, Canada) or the Jazz Integra Wireless Headset (Ober Consulting, Poznan, Poland) and sampled at 1 ms intervals. The stimulus was a white circular target on a black background; background room luminance was 6-12 candela to improve compliance with recording. The stimulus sequence consisted of cycles in which each target was displayed for 20 seconds in primary position and  $\pm 15^\circ$  horizontally and then repeated at  $\pm 15^\circ$  vertically. The head was stabilized in the primary position using a chin rest. Calibration was performed so that the foveating periods of the waveform were fixated on the targets at  $15^\circ$ . Where the waveform was a pure pendular subtype (ie, without a foveating period), fixation was taken as the median position of the cycle. Analysis routines were implemented using the software package Mathematica (Wolfram Research, Inc., Champaign, IL).<sup>10</sup>

Waveforms were classified according to the CEMAS Working Group,<sup>11</sup> with infantile nystagmus waveforms defined by the presence of at least one accelerating exponential slow phase, and fusion maldevelopment nystagmus syndrome (FMNS) waveforms defined by the presence of at least one decelerating exponential slow phase. Where the waveform was pure pendular (ie, sinusoidal with no slow phase), this was documented. Waveforms were described simply in terms of frequency, mean vertical and horizontal amplitude, and phase disparity, as described by Gottlob and Reinecke.<sup>12</sup>

### *SD-OCT*

Standard table-mounted SD-OCT imaging was performed on both eyes, following pupillary dilation with tropicamide 1% and phenylephrine 2.5% eye drops in adults, or cyclopentolate 0.5% in subjects <10 years of age. Line and volume retinal scans were acquired with the Spectralis device (Heidelberg Engineering, Heidelberg, Germany). Qualitative assessment of foveal structure was performed by grading SD-OCT images according to the five categories described by Sundaram and colleagues,<sup>13</sup> with the term *ellipsoid zone* (EZ) used instead of the authors' *inner segment ellipsoid layer*<sup>14</sup>: (1) continuous photoreceptor EZ, (2) EZ disruption, (3) EZ absence, (4) presence of a hyporeflective zone (HRZ), and (5) outer retinal atrophy including retinal pigment epithelium loss. The EZ is identified as the second hyper-reflective band of the outer retina and is located just below the external limiting membrane on SD-OCT. It is normally a continuous smooth line of homogenous reflectivity. EZ disruption indicates irregularity of this band at the fovea, with loss of an even contour and variation in reflectivity. EZ absence is complete loss of a section of this hyper-reflective band at the fovea, without the presence of an associated HRZ. The presence of an HRZ indicates complete loss of a section of the EZ at the fovea, associated with a hypo-reflective (black) area between the region of EZ loss and the

external limiting membrane above.

A number of techniques were used to minimize nystagmus-related artefacts on the scans. Subjects who could voluntarily control their nystagmus were encouraged to do so during scanning. Those who found it difficult to maintain a steady gaze were asked to fixate on an external target (a white light) attached to the scanning device. They were instructed to focus on the target with one eye while the fellow eye was scanned in order to damp nystagmus. With regard to the scanning protocol, in subjects with severe nystagmus, images were acquired in high-speed mode as opposed to high-resolution mode. Furthermore, the automatic real-time function on the device (which aims to ensure that all B-scans required to cover the imaging area of interest are acquired coherently despite eye movements) was turned off. Signal strength was defined as a quality score. The Spectralis device automatically generates a quality score of 0–40 dB for each scan, and only images with a quality score of  $\geq 25$  dB were deemed acceptable.

## Results

A total of 18 subjects (5 males) were included: 11 adults and 7 children (8–13 years of age). The mean age at time of review was 19.4 years (range, 8–33 years). The mean best-corrected visual acuity was 0.78 logMAR in the right eye (range, 0.46–1.02 logMAR) and 0.79 logMAR in the left eye (range, 0.5–1.02 logMAR). The Snellen equivalent of the mean best-corrected visual acuity was 20/120 in the right eye (range, 20/58–20/209) and 20/123 in the left eye (range, 20/63–20/209). Mean refractive error (spherical equivalent) was +1.45 D in the right eye (median, +1.25D; range, –5.25 to +7.25 D) and +1.48 D in the left eye (median, +1.25 D; range, –9.00 to +6.625D). Table 1 summarizes patient characteristics and baseline clinical findings. In all subjects, fundus appearance was normal bilaterally, with no obvious macular abnormalities.

### *Assessment of Eye Movements*

Table 2 summarizes eye movement findings. The majority of subjects demonstrated a phoria; manifest strabismus was present in only 3 subjects. With regard to nystagmus findings, subject 12 was excluded from analysis because of noisy recordings. The predominant nystagmus waveform was decided using a combination of two techniques, depending on the duration of eye movement recording.<sup>10,15</sup> The method of closed returns is a visual technique that allows for the identification of periodicities by plotting the differences between the eye position at time  $t$ , and some other time  $t + dt$ , over a range of time differences, with the difference plotted on a gray scale. This makes it easy to identify the segment of data where the waveform cycle length is approximately uniform, correlating to the predominant waveform.<sup>10,16</sup> The second method, periodic orbit analysis, uses a four-step technique to identify the underlying periodicity of the waveform, which correlates with the predominant waveform.<sup>10,17</sup>

The predominant waveform, present in the 17 subjects with usable recordings, was pure pendular. Nine subjects demonstrated a mixture of waveforms with more than one subtype present. A combination of accelerating and decelerating exponential slow phases was seen in 5 subjects, reflecting a mixture of INS and FMNS. Of the 9, an increasing velocity slow phase was seen in 3 subjects; a decreasing velocity slow phase in 1.

Subjects 2 and 14 had alternating exotropias. They had a combination of pure pendular and jerk nystagmus waveforms, with both increasing and decreasing exponential slow velocity phases. Subjects 1, 7, and 13 were phoric and had combined pure pendular and jerk waveforms, with both increasing and decreasing exponential slow velocity phases. Subject 3 was phoric and had a combination of pure pendular and jerk waveforms, with decreasing exponential slow velocity phases. The FMNS waveform subtype was present in all of these subjects but was not the predominant waveform. Although FMNS is typically associated with early-onset strabismus,



it has been documented to occur in large phorias and in individuals with variable stereopsis.<sup>18</sup> A decreasing velocity slow phase has also been documented in some of the orthotropic achromatopsia subjects described by Gottlob and Reinecke.<sup>12</sup>

All subjects had a vertical element to their nystagmus (ie, oblique nystagmus seen on the horizontal and vertical channels during eye movement recordings). However, the horizontal amplitude was typically greater than the vertical amplitude. Nystagmus frequencies varied from 4 to 8 cycles/second. The waveforms were in phase in 12 of 17 subjects, in and out of phase in 4, and out of phase throughout the entire recording in only 1 subject. There were no notable differences in eye movements between adults and children.

#### *SD-OCT Findings*

Scans with a quality score of  $\geq 25$  dB were obtained from all subjects. SD-OCT imaging of the retina revealed a continuous EZ in 2 of 18 subjects (grade 1) and EZ disruption in 16 (grade 2). Retinal structure characteristics were symmetrical, with the same grade recorded bilaterally in each individual. No subjects had an SD-OCT grade of 3 or worse.

Representative nystagmus waveforms and SD-OCT images are provided in Figures 1 and 2. Subject 6 (Figure 1) demonstrated high-frequency and low-amplitude torsional nystagmus. Subject 16 (Figure 2) had a high-frequency and low-amplitude pendular nystagmus waveform superimposed on a larger jerk waveform. Both subjects showed disruption of the EZ at the fovea (grade 2) on SD-OCT.

#### **Discussion**

This is the largest study to date of achromatopsia subjects in terms both of total cohort and number of adults. In concordance with the work of Gottlob and Reinecke,<sup>12</sup> we found that the amplitudes and frequencies of the nystagmus waveforms were symmetrical between eyes in each

individual, with both horizontal and vertical components to the waveform in all subjects. There was no obvious correlation between nystagmus speed or form and a subject's visual acuity. There are, however, notable differences between our results and those of Gottlob and Reinecke.<sup>12</sup> It is difficult to be certain whether our cohort truly differed from theirs in terms of severity, because SD-OCT was unavailable at the time of their study. Gottlob and Reinecke<sup>12</sup> reported that a jerk waveform predominated in adults<sup>12</sup>; we, on the contrary, observed pendular nystagmus to be universal in our cohort and the predominant waveform overall. It could be that the subjects in our study were younger; it is believed that subjects with INS acquire the more common jerk waveforms (with foveating advantages) with age.<sup>19</sup> Additionally, the Gottlob and Reinecke cohort was likely more heterogeneous than ours, and so the two groups of subjects may not be directly comparable in terms of the extent of retinal disruption.

Although the frequencies we recorded were similar in range to what Gottlob and Reinecke<sup>12</sup> reported, the overall amplitudes we observed were smaller (ie, suggestive of very fine nystagmus). This may be attributed to our use of a noncontact eye tracking system, which is better tolerated than the magnetic search coil technique used in earlier work and is thus less likely to cause a worsening of nystagmus.<sup>20</sup> It is also feasible that the smaller amplitudes observed in our group may be a result of our subjects having lesser degrees of retinal disruption than those in the Gottlob and Reinecke study,<sup>12</sup> which was conducted prior to OCT classification. Of note, the subjects within our cohort were at the milder end of the spectrum with regard to SD-OCT appearance; hence, finer nystagmus may perhaps be a feature of less retinal disruption at the fovea. This may account for the universal finding of low-amplitude pendular nystagmus in our subjects, ie, the less-disrupted fovea precludes the development of foveation strategies to utilize extrafoveal regions. Further work investigating eye movements in achromatopsia subjects

with more marked SD-OCT disturbance may help establish whether there is a correlation between the severity of nystagmus and the extent of retinal disruption, although no difference was observed between our subjects with normal structure (grade 1) and mild disruption (grade 2); however, only 2 subjects had grade 1 SD-OCT appearances. It has been suggested that nystagmus becomes damped with age in achromatopsia.<sup>21</sup> Our study supports the findings of Gottlob and Reinecke<sup>12</sup> in showing no marked difference between adults and children in the frequency or amplitude of waveform.

Our results suggest that nystagmus in achromatopsia is symmetrical between an individual's eyes with regard to frequency and amplitude (amplitude typically  $<2^\circ$ ) and has horizontal and vertical elements. Furthermore, it may be disconjugate. These characteristics may enable nystagmus secondary to achromatopsia to be distinguished from other forms of nystagmus, which differ in these parameters.<sup>22</sup> Typically, infantile nystagmus is conjugate, predominantly horizontal, and of larger amplitude (particularly in early infancy). If a patient presented with any other profile, investigation for an underlying neurological cause would ensue. Our results highlight the importance of considering retinal disease in an otherwise well infant presenting with atypical nystagmus. In addition to ocular motility findings, we present the foveal SD-OCT appearances of our subjects. The retina in achromatopsia frequently appears normal on clinical examination, but detailed imaging typically reveals abnormalities in the integrity of the photoreceptor layer at the fovea.<sup>8,23,24</sup> The structural changes in the retina vary in severity, and of note, the subjects in our cohort were at the mild range of the spectrum, with 2 subjects showing no significant disruption of the photoreceptor layer, and the remainder showing relatively mild disruption. Notably however, our patients were those selected to participate in a gene therapy trial for *CNGB3*-associated achromatopsia. In accordance with the trial inclusion criteria, only

those individuals with grade 1 or grade 2 SD-OCT images were selected. More marked abnormalities of the photoreceptor layer may be observed in subjects with achromatopsia, and foveal hypoplasia may be an additional feature on SD-OCT.<sup>13,25-27</sup> Further studies investigating subjects with achromatopsia who have more extensive retinal disturbance (grade 3 or higher on SD-OCT) may shed new light on whether there is a correlation between the extent of retinal disruption and various parameters of visual function, including the type and severity of nystagmus.

Our study has several limitations. First, our sample size of 18 subjects is relatively small, and our results may not be generalizable to a wider population of affected individuals. Second, our cohort did not include young babies and children of the age where an underlying diagnosis would typically be sought in cases of infantile nystagmus. We note, however, that a recent work investigating changes in retinal structure in a large cohort of subjects with achromatopsia over an extended time period has demonstrated that structural appearances are relatively stable over time.<sup>25,26</sup> Accordingly, we have assumed that the retinal abnormalities observed in our cohort of older subjects would have been similar to those manifested earlier in their childhood. Finally, our study included only those with *CNGB3*-associated achromatopsia. It is possible that different nystagmus characteristics may be observed in individuals that have achromatopsia secondary to alternative genetic variants. Further work assessing nystagmus in a genotypically heterogeneous cohort of affected individuals may demonstrate this.

In spite of these limitations, our findings suggest that SD-OCT may aid the diagnosis of achromatopsia in young individuals with nystagmus and that early establishment of retinal disease as the underlying cause may eliminate the need for further, more invasive investigations. This principle may be applied to ocular motility abnormalities arising from a range of ocular

disorders. Bertsch and colleagues<sup>3</sup> found that retinal disorders were the most common cause of infantile nystagmus in their pediatric cohort, and yet MRI of the brain was the most common first-line imaging. In practice, this may in part be attributed to difficulties obtaining adequate SD-OCT imaging, particularly in infants. However, the authors concluded that retinal imaging may have a higher yield in patients without other neurological signs and thus advocated its use at an earlier stage in the work-up for nystagmus.

SD-OCT has been used to identify the morphologic features of a range of retinal dystrophies associated with nystagmus, including retinitis pigmentosa, Leber congenital amaurosis, and cone or cone-rod dystrophies and has enabled the identification of a range of retinal disorders in children with nystagmus, including albinism and retinal dystrophy associated with *PAX6* mutations, in addition to achromatopsia.<sup>4</sup> A spectrum of foveal morphological abnormalities have been identified with SD-OCT in subjects with ocular albinism or suspected ocular albinism and nystagmus. These anomalies include the persistence of an abnormal, highly reflective band across the fovea, the presence of multiple inner retinal layers normally absent at the center of the fovea, and the loss of the normally thickened photoreceptor nuclear layer at the fovea.<sup>28</sup> Subjects with *PAX6* mutations generally show foveal hypoplasia similarly but usually less severely than that seen in albinism.<sup>5</sup>

SD-OCT may unmask retinal disease in patients previously diagnosed with idiopathic congenital nystagmus or unexplained/functional visual loss.<sup>29</sup> It is particularly important in establishing a diagnosis in retinal conditions, including achromatopsia, where there may be no significant abnormality on fundus examination and in conditions that may have a wide expressivity and heterogeneity, such as albinism. Accurate diagnosis will allow better overall management, including optimal visual rehabilitation, informed advice on the course and

prognosis of the disease, and prioritization of genetic testing and counselling where appropriate.

Prompt diagnosis is increasingly important in an era where potential gene therapies for inherited retinal disorders are emerging, and where early intervention is considered key.

Journal Pre-proof

## References

1. Hussain N. Diagnosis, assessment and management of nystagmus in childhood. *Paediatrics and Child Health* 2016;26:31-6.
2. Sarvananthan N, Surendran M, Roberts EO, et al. The prevalence of nystagmus: the Leicestershire nystagmus survey. *Invest Ophthalmol Vis Sci* 2009;50:5201-6.
3. Bertsch M, Floyd M, Kehoe T, Pfeifer W, Drack AV. The clinical evaluation of infantile nystagmus: what to do first and why. *Ophthalmic Genet* 2017;38:22-33.
4. Papageorgiou E, McLean RJ, Gottlob I. Nystagmus in childhood. *Pediatr Neonatol* 2014;55:341-51.
5. Lee H, Sheth V, Bibi M, et al. Potential of handheld optical coherence tomography to determine cause of infantile nystagmus in children by using foveal morphology. *Ophthalmology* 2013;120:2714-24.
6. Lee H, Proudlock F, Gottlob I. Is handheld optical coherence tomography reliable in infants and young children with and without nystagmus? *Invest Ophthalmol Vis Sci* 2013;54:8152-9.
7. Yang P, Michaels KV, Courtney RJ, et al. Retinal morphology of patients with achromatopsia during early childhood: implications for gene therapy. *JAMA Ophthalmol* 2014;132:823-31.
8. Hirji N, Aboshiha J, Georgiou M, Bainbridge J, Michaelides M. Achromatopsia: clinical features, molecular genetics, animal models and therapeutic options. *Ophthalmic Genet* 2018;39:149-57.
9. Aboshiha J, Dubis AM, Carroll J, Hardcastle AJ, Michaelides M. The cone dysfunction syndromes. *Br J Ophthalmol* 2016;100:115-21.

10. Theodorou M. Nystagmus and Visual Acuity [PhD thesis]. London: Institute of Child Health, University College London; 2009.
11. CEMAS Working Group. The Classification of Eye Movement Abnormalities and Strabismus (CEMAS). The National Eye Institute Publications ([www.nei.nih.gov](http://www.nei.nih.gov)). Bethesda, MD: The National Eye Institute, The National Institutes of Health; 2001.
12. Gottlob I, Reinecke RD. Eye and head movements in patients with achromatopsia. *Graefes Arch Clin Exp Ophthalmol* 1994;232:392-401.
13. Sundaram V, Wilde C, Aboshiha J, et al. Retinal structure and function in achromatopsia: implications for gene therapy. *Ophthalmology* 2014;121:234-45.
14. Tao LW, Wu Z, Guymer RH, Luu CD. Ellipsoid zone on optical coherence tomography: a review. *Clin Exp Ophthalmol* 2016;44:422-30.
15. Theodorou M, Clement R, Taylor D, Moore A. The development of infantile nystagmus. *Br J Ophthalmol* 2015;99:691-5.
16. Mindlin GB, Solari HG, Natiello MA, Gilmore R, Hou X-J. Topological analysis of chaotic time series data from the Belousov-Zhabotinskii reaction. *J Nonlinear Sci* 1991;1:147-73.
17. Theodorou M, Clement RA. Fixed point analysis of nystagmus. *J Neurosci Methods* 2007;161:134-41.
18. Gresty MA, Metcalfe T, Timms C, Elston J, Lee J, Liu C. Neurology of latent nystagmus. *Brain* 1992;115:1303-21.
19. Reinecke RD. Costenbader Lecture. Idiopathic infantile nystagmus: diagnosis and treatment. *J AAPOS* 1997;1:67-82.
20. Ganança MM, Caovilla HH, Ganança FF. Electronystagmography versus



- videonystagmography. *Braz J Otorhinolaryngol* 2010;76:399-403.
21. Zobor D, Zobor G, Kohl S. Achromatopsia: on the doorstep of a possible therapy. *Ophthalmic Res* 2015;54:103-8.
  22. Abadi RV, Bjerre A. Motor and sensory characteristics of infantile nystagmus. *Br J Ophthalmol* 2002;86:1152-60.
  23. Thomas MG, Kumar A, Kohl S, Proudlock FA, Gottlob I. High-resolution in vivo imaging in achromatopsia. *Ophthalmology* 2011;118:882-7.
  24. Thomas MG, Gottlob I. Optical coherence tomography studies provides new insights into diagnosis and prognosis of infantile nystagmus: a review. *Strabismus* 2012;20:175-80.
  25. Aboshiha J, Dubis AM, Cowing J, et al. A prospective longitudinal study of retinal structure and function in achromatopsia. *Invest Ophthalmol Vis Sci* 2014;55:5733-43.
  26. Hirji N, Georgiou M, Kalitzeos A, et al. Longitudinal assessment of retinal structure in achromatopsia patients with long-term follow-up. *Invest Ophthalmol Vis Sci* 2018;59:5735-44.
  27. Langlo CS, Patterson EJ, Higgins BP, et al. Residual foveal cone structure in CNGB3-associated achromatopsia. *Invest Ophthalmol Vis Sci* 2016;57:3984-95.
  28. Chong GT, Farsiu S, Freedman SF, et al. Abnormal foveal morphology in ocular albinism imaged with spectral-domain optical coherence tomography. *Arch Ophthalmol* 2009;127:37-44.
  29. Holmström G, Bondeson ML, Eriksson U, Åkerblom H, Larsson E. "Congenital" nystagmus may hide various ophthalmic diagnoses. *Acta Ophthalmol* 2014;92:412-16.

## Legends

**FIG 1.** Representative nystagmus waveform and spectral domain optical coherence tomography (SD-OCT) from subject 6. Horizontal (A) and vertical position (B) profiles of the right eye. The nystagmus was of the pure pendular subtype, out of phase and with a small amplitude (mean,  $<1^\circ$ ) and high frequency (6-8 cycles/sec). Horizontal and vertical elements were approximately equal. Disruption of the ellipsoid zone at the fovea may be seen in the lower panel (grade 2, white arrow).

**FIG 2.** Representative nystagmus waveform and SD-OCT image from subject 16. Horizontal and vertical position profiles (upper and middle figures, respectively) of the left eye. The nystagmus was a mixture of in and out of phase, pure pendular and dual jerk subtype (dual jerk shown for example). The jerk subtype was of moderate amplitude (mean,  $4.7^\circ$  horizontal plane;  $3.2^\circ$  vertical plane) with a higher frequency pendular waveform superimposed on the slow phase. The lower figure shows disruption of the ellipsoid zone at the fovea (grade 2, white arrow).

Table 1. Summary of patient characteristics and clinical findings

Subject	Sex	Age, years	BCVA, logMAR		Refraction		SE, D		SD-OCT grade <sup>a</sup>	
			Right eye	Left eye	Right eye	Left eye	Right eye	Left eye	Right eye	Left eye
1	M	30	0.86	0.80	+4.50 -0.50 x70	+4.00 -1.00 x95	+4.25	+3.50	2	2
2	F	18	0.70	0.64	+4.00 -1.50 x90	+3.50 -0.50 x120	+3.25	+3.25	2	2
3	F	24	0.74	0.78	+1.75 -1.75 x180	+2.75 -3.00 x180	+0.875	+1.25	2	2
4	F	33	0.78	0.78	+4.75 -3.00 x65	+3.75 -2.00 x80	+3.25	+2.75	2	2
5	F	18	0.68	0.72	-1.00	+1.00	-1.00	+1.00	2	2
6	F	26	0.78	0.82	+0.50 -2.00 x125	-1.25	-0.50	-1.25	2	2
7	F	30	0.88	0.86	-4.50	-9.00	-4.50	-9.00	2	2
8	M	30	0.76	0.76	-4.25 -2.00 x180	-1.50 -0.50 x180	-5.25	-1.75	2	2
9	F	21	0.46	0.50	-0.75 -1.00 x180	Plano/+0.25 x30	-1.25	+0.125	1	1
10	F	16	0.70	0.74	+0.50 -0.25 x5	+0.75 -0.25 x175	+0.375	+0.625	2	2
11	M	12	1.02	1.02	+3.50 -1.00 x145	+7.00 -0.75 x120	+3.00	+6.625	1	1
12	F	9	0.82	0.82	+1.00	+0.75 -0.50 x40	+1.00	+0.50	2	2
13	M	22	0.78	0.78	-0.50 -0.50 x110	-1.50	-0.75	-1.50	2	2
14	F	13	0.84	0.90	+6.25 -2.00 x180	+7.00 -2.50 x180	+5.25	+5.75	2	2
15	M	13	0.78	0.82	+8.00 -1.50 x180	+4.25 -1.00 x180	+7.25	+3.75	2	2
16	F	13	0.94	0.86	+2.00 -1.00 x110	+1.75 -1.00 x70	+1.50	+1.25	2	2
17	F	13	0.76	0.70	+5.50 -3.00 x180	+7.50 -3.00 x145	+4.00	+6.00	2	2
18	F	8	0.80	0.86	+6.00 -1.25 x170	+4.50 -1.25 x160	+5.375	+3.875	2	2

BCVA, best-corrected visual acuity; SD-OCT, spectral domain optical coherence tomography; SE, spherical equivalent.

<sup>a</sup>SD-OCT grade: 1, continuous ellipsoid zone (EZ); 2, EZ disruption; 3, EZ absence; 4, HRZ present; 5, outer retinal atrophy.

Table 2. Summary of eye movement findings

Subject	Orthoptic findings	Predominant waveform	Nystagmus findings			
			Mean amplitude, deg		Frequency of predominant waveform, cycles/sec	Phase disparity
			Horizontal	Vertical		
1	X	Pure P; J, incr/decr vel	<2	<2	4-6	In phase
2	Alternating XT (moderate)	Pure pendular; jerk, incr/decr vel	2-4	<2	4-6	In phase
3	X	Pure P; J, decr vel	<2	<2	4-6	In phase
4	X	P; J, incr vel	<2	<2	4-6	In phase
5	X	Pure P	<2	<2	4-6	In phase
6	E	Pure P	<2	<2	6-8	Out of phase
7	E	Pure P; J, incr/decr vel	<2	<2	4-6	In phase
8	X	Pure P	2-4	<2	4-6	In phase
9	X	Pure P	<2	<2	4-6	In phase
10	X/E	Pure P	<2	<2	4-6	In phase
11	X	Pure P	<2	<2	4-6	In phase
12	X	Pure P	N/A	N/A	N/A	In phase
13	X/E	Pure P; J, incr/decr vel	<2	<2	4-6	In/out of phase
14	Alternating XT (moderate)	Pure P; J, incr/decr vel	4-6	4-6	6-8	In phase
15	E + primary IOOA	Pure P; J, incr vel	>6	<2	4-6	In phase
16	XT/ET (small)	Pure P; J, incr vel	4-6	2-4	4-6	In/out of phase
17	X + secondary IOOA	Pure P	<2	<2	4-6	In/out of phase
18	X	Pure pendular	<2	<2	4-6	In/out of phase

*Decr*, decreasing; *E*, esophoria; *ET*, esotropoia; *Incr*, increasing; *IOOA*, inferior oblique overaction; *J*, jerk; *N/A*, not available; *P*, pendular; *Vel*, velocity; *X*, exophoria; *XT*, exotropia.

